Liquid Phase Deposition Based SnO_2 Gas Sensor Integrated With TaN Heater on a Micro-Hotplate

Jin-Chern Chiou, *Member, IEEE*, Shang-Wei Tsai, and Chia-Yang Lin

***Abstract*— A micromachined liquid-phase deposition (LPD)-based SnO_2 gas sensor that is integrated with a tantalum nitride (TaN) microheater on micro-hotplate is designed and fabricated using microelectromechanical systems technology. TaN is available in many traditional complementary metal oxide semiconductor designs, unlike many other microheater materials. For the initial time, TaN is used in semiconductor metal oxide gas sensor as a heater. The thermal response, thermal distribution, and power consumption of the TaN microheater are measured using a thermal imaging camera. The operating temperature of TaN micro-hotplate can exceed 500 °C and they have a favorable thermal distribution within the sensing area. The temperature variation over the sensing area for a TaN microheater with a size of 300 × 300 μm is ∼4% at 500 °C. Its power consumption is successfully decreased by adopting a structure with ratio of edge length of the membrane to that of the microheater of 2.5. The sensing responses of the LPD-based SnO_2 gas sensor with the TaN microheater to H_2S gas are measured at various operating temperatures. The optimal operating temperature of the designed gas sensors is in the range 250 °C–300 °C. The designed sensing film with an area of 100 × 100 μm has greater sensitivity to a staircase concentration of H_2S gas than those with the other two areas (200 × 200 μm and 300 × 300 μm).**

***Index Terms*— MEMS, micro-hotplate, micro-heater, tin oxide, gas sensor, liquid phase deposition.**

I. Introduction

MICROELECTROMECHANICAL system (MEMS)-based micro-hotplates generally consist of a thin film heater coil or wire, which can provide high temperatures at low power consumption and exhibit a fast thermal response time. In recent years, MEMS-based micro-hotplates have been increasingly used in gas sensors [1]–[3]. Si-based micromachined gas sensors are highly promising because their fabrication procedure is compatible with the integrated circuit (IC) process, enabling sensors and signal conditioning to be integrated with each other. Specialized micro-hotplate devices were developed using micromachining technology in the early 1990s. In 1993, the National Institute of Standards and Technology (NIST) pioneered the notion of markedly reducing the power consumption of gas sensors by means of micro-hotplate technology [4]. The advantages of MEMS micro-hotplates are their fast thermal response time and their being able to reach high temperatures with low power consumption. Additionally, the use of a micro-hotplate in a gas sensor can improve the dynamic response in the sensing process and reduce the power consumption. In a gas sensor, the heating uniformity and stability of micro-heater are important in the sensing process as they affect the sensitivity and selectivity of the sensor. More uniform heating of a sensing film is associated with a better interaction between grains and gas molecules and greater sensitivity. Hence, a high temperature should be maintained uniformly across the active region.

Poly-silicon (poly-Si) and platinum (Pt) are the materials that are most commonly used in micro-heaters and thermometers. Poly-Si was the first material used in micro-heater and can be easily integrated in an IC-process. However, when such a device operates at high temperature, its resistance becomes unstable [5]. Pt is now the most popular material for use in micro-heaters because of its stable temperature coefficient of resistance, tolerance of large current densities, and high melting point (1768 °C) [6]. However, it is nonstandard in ICs. This investigation studies tantalum nitride (TaN) as an alternative material for use in micro-heaters. In the past, TaN has been used as thin-film resistors. It has many appealing characteristics, such as a negative and small TCR, high sheet resistance, high melting point (3090 °C), chemical inertness and hardness [7]–[10]. For these reasons, in this work, TaN is used as a new material in a micro-heater and integrated with a micro-hotplate, providing the advantages of high sensitivity, high robustness and a miniaturized structure.

In this work, a micromachined LPD-based Tin-Oxide (SnO_2) gas sensor with TaN micro-heater is designed and fabricated and an earlier version of this paper was presented at the IEEE Sensors Conference and was published in its

Manuscript received December 13, 2012; revised February 17, 2013 and March 29, 2013; accepted March 29, 2013. Date of publication April 4, 2013; date of current version April 30, 2013. This work was supported in part by the National Science Council, Taiwan, and "Aim for the Top University Plan" of the National Chiao Tung University and Ministry of Education, Taiwan. This work was also particularly supported by R&D Piloting Cooperation Projects between Industries and Academia at Science Parks under Contract 100A20, the Technology Development Program for Academia sponsored by Ministry of Economic Affairs under Contract 101-EC-17-A-01-S1-180 and the UST-UCSD International Center of Excellence in Advanced Bioengineering sponsored by the Taiwan National Science Council I-RiCE Program under Grant NSC-101-2911-I-009-101. The associate editor coordinating the review of this paper and approving it for publication was Dr. Anupama Kaul.

J.-C. Chiou is with the Department of Electrical Engineering, National Chiao Tung University, Hsinchu 30010, Taiwan. He is also with the Biomedical Engineering Research and Development Center of China Medical University, Taichung 40402, Taiwan (e-mail: chiou@mail.nctu.edu.tw).

S.-W. Tsai is with the Department of Electrical Engineering, National Chiao Tung University, Hsinchu 30010, Taiwan (e-mail: shangwei916@gmail.com).

C.-Y. Lin was with the Institute of Electrical and Control Engineering, National Chiao Tung University, Hsinchu 30010, Taiwan. He is now with United Microelectronics Corporation, Tainan 744, Taiwan (e-mail: kylelin99.ece99g@nctu.edu.tw).

Color versions of one or more of the figures in this paper are available online at http://ieeexplore.ieee.org.

Digital Object Identifier 10.1109/JSEN.2013.2256780

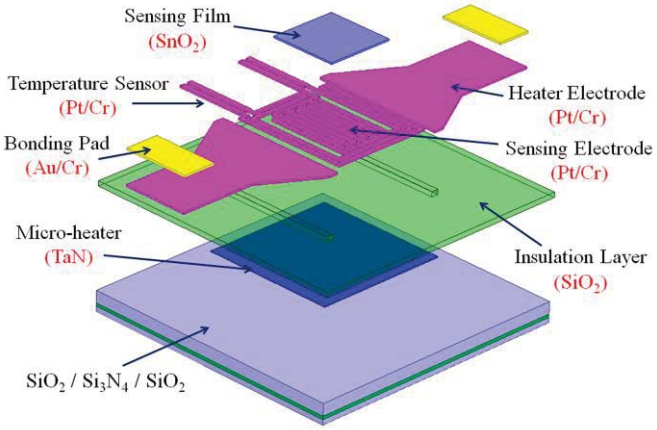

Fig. 1. Exploded 3-D schematic of functional layers in the micromachined micro-hotplate.

proceedings [11]. Three ratios of the edge length of the membrane to that of micro-heater are designed to determine the effect of that ratio on power consumption. The thermal distributions of the micro-hotplates when they were heated by a TaN micro-heater are also measured. Finally, the responses of the micromachined SnO_2 gas sensor at various operating temperatures to various concentrations of H_2S were measured and discussed.

II. Design and Fabrication

A. Design of Micromachined SnO_2 Gas Sensor

Fig. 1 shows the 3-D schematic of the micro-hotplate-based gas sensor of closed-membrane type. The micromachined gas sensor consists of a TaN-based micro-heater, platinum-based interdigital electrodes and a thermometer, and a SnO_2 sensing film, prepared by liquid phase deposition (LPD). The LPD method is defined as the film can be deposited by using the method of deriving the hydrolysis oxides from MF_6^{2-} ion (M = Ti, Sn, Si) in H_2MF_6 solution. The reaction of the hydrolysis oxide is based on the ligand-exchange hydrolysis of a metal-fluoro complex ($MF_x^{(x-2n)-}$) and an F^- consumption reaction with boric acid or aluminum metal [12]. The size of the gas sensor device is 3200 μm × 3200 μm and TaN micro-heaters are designed with areas of 300 μm × 300 μm, 400 μm × 400 μm and 500 μm × 500 μm.

The micro-heater is sandwiched between the released $SiO_2/Si_3N_4/SiO_2$ (O/N/O) membrane and SiO_2 film. This structure provides electrical and chemical isolation from the atmosphere, and effective thermal isolation of the membrane rim. When platinum is used as the electrode material, the sensor electrode and the structure of the thermometer can be integrated in a single layer.

The micro-hotplate based on the closed membrane in the design herein looses heat mainly by natural convection: much less heat is lost by conduction and radiation [13]. This means that the change of thermal resistance in the environment depends mainly on the geometry of the micro-hotplate and is independent of the heater material. Therefore, micro-hotplates with the released membranes of various sizes were utilized to analyze the power consumption of the micro-heater at various temperatures. Fig. 2 shows a simple model of the design of the closed-membrane and micro-heater. The symbols of "a", "b" and "d" denote a edge length of the square membrane, a edge length of the square heating resistor and thickness of the square membrane, respectively. According to the geometry property shown in Fig. 2, in this work, the designs use ratios of the edge length of the O/N/O membrane to that of the micro-heater of 2, 2.5 and 3.

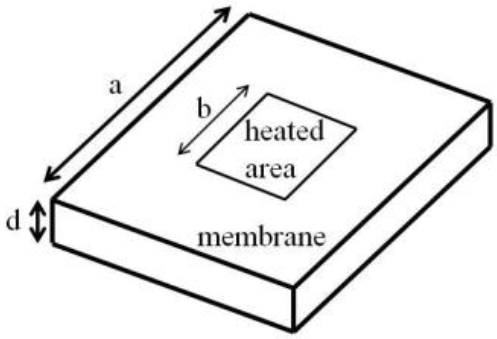

Fig. 2. The schematic design of the membrane and the micro-heater.

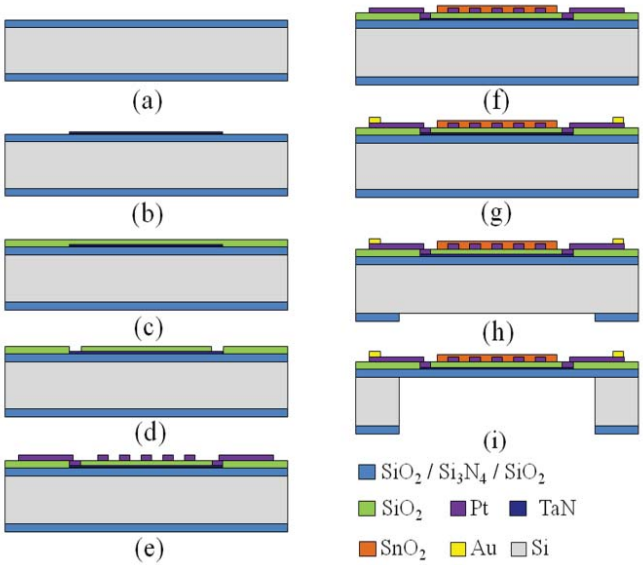

Fig. 3. Schematic flow of micromachining process for micromachined SnO_2 gas sensor.

B. Fabrication and Measurement of Properties of Micromachined SnO_2 Gas Sensor

Fig. 3 shows the flow of micromachining process that involves the designed gas sensor. The starting material was a 4 inch, 250 μm-thick, p-type, <100>-oriented, double polished silicon wafer. In Fig. 3(a), first, The wafers were covered by 300 nm wet thermal oxide, 200 nm low-stress silicon nitride (Si_3N_4), deposited by low power chemical vapor deposition (LPCVD) at 850 °C, and 700 nm SiO_2, deposited by plasma enhanced chemical vapor deposition (PECVD) on the front-side and backside. The front layer was a part of the micro-hotplate structure, while the backside layer was used as a hard mask for inductively coupled plasma (ICP) etching.

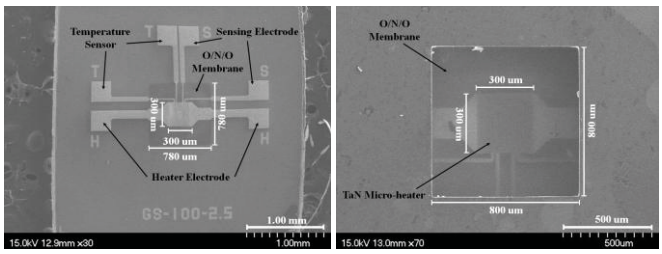

(a) (b)

Fig. 4. SEM micrographs of micromachined SnO_2 gas sensor: (a) front side and (b) back side.

In the Fig. 3(b), a 50 nm thickness of TaN was deposited on the front of the substrate by sputtering in an Ar/N_2 gas mixture and patterned as micro-heater using high density plasma reactive ion etching (HDP-RIE). The $N_2/(Ar+N_2)$ gas flow ratio in this investigation was 5 %, and the composition ratio of Ta/N was approximately one. In the Fig. 3(c)–(d), after deposition of the TaN micro-heater, a SiO_2 film with a thickness of 300 nm was deposited by PECVD as an isolation layer between the micro-heater and the electrodes. Then the contact window to the micro-heater was opened by HDP-RIE. Next, In the Fig. 3(e), an adhesive layer of 20 nm chromium (Cr), followed by a 100 nm-thick layer of Pt was deposited by sputtering and patterned using a lift-off process to form the electrodes of the sensing layer, micro-heater and temperature sensor.

The sensing area of the Tin-Oxide (SnO_2) was defined using a patterned photoresist on the interdigital Pt electrode as shown in Fig. 3(f). The porous SnO_2 sensing film was deposited on the sensing area by liquid phase deposition (LPD). The growth solution for LPD method was prepared by mixing the dissolved SnF_2 powder in deionized (DI) water and the saturated H_2SiF_6 solution, and which the molar ratio of Si:Sn was maintained at 1:3. Then the silicon substrates were vertically immersed in the solution for ten hours at 60 °C with stirring to deposit the SiO_2-doped SnO_2 film. The details of the fabrication process have been presented elsewhere [14].

After deposition, the photoresist was removed using acetone to yield a patterned SnO_2 film. The sensing film was then calcined at 600 °C for one hour in air and formed the rutile phase of SnO_2. The atomic concentrations of Sn and Si in the deposited film are 29.03 % and 2.44 %, respectively. In the Fig. 3(g), an adhesion layer of 30 nm Cr and then 300 nm Au were deposited by sputtering, and patterned by the lift-off method as the conducting wire of the micro-heater and the bonding pad. In the Fig. 3(h)–(i), on the backside, the O/N/O membrane was opened by HDP-RIE into an etching window. Finally, the closed-membrane structure was released by ICP etching from the backside and the O/N/O membrane was used as a hard mask to protect the silicon substrate from attack during the etching process. Fig. 4 presents the results of fabricating the micromachined SnO_2 gas sensor.

The TaN layer was characterized in terms of the temperature coefficient of the resistance (TCR) and the heating properties of the micro-hotplate. The resistance of the heater was measured using a source monitor unit at temperatures from room temperature up to 300 °C in the isothermal water bath. The heating characteristics of the TaN micro-heater were measured using a thermal imaging camera (A320) from FLIR System. The range of the infrared spectrum of the thermal imaging camera that was used in making measurements was between 7.5 μm and 13 μm and the camera was able to measure temperatures above 1200 °C. The thermal distribution and temperature variation of the heated micro-heater were evaluated by measuring the maximum and minimum temperatures within the sensing area.

To determine the gas-sensing properties of the micromachined SnO_2 sensor, the sensing films with sizes of 100 μm × 100 μm, 200 μm × 200 μm and 300 μm × 300 μm were placed in a test chamber at room temperature. Their resistance (R_a) in air was measured using a conventional circuit in which the sensor was connected in series to an external resistor, with a circuit voltage of 1.5V. The response to H_2S was obtained by injecting various concentrations of the H_2S gas into the chamber and measuring the resistance (R_g) of the sensor. The response of each sensor to staircase concentrations of H_2S gas was measured by recording the resistance of the sensor.

III. Results and Discussion

A. Thermal Characteristics of TaN-Based Micro-Heater

The temperature coefficient of resistance (TCR) of the TaN films was measured using an isothermal water bath, which was fabricated in a chip size and mounted on a metal plate with four leads as electrical connection and then sealed with a metal cap by high-current wilding (known as the TO-Can package). First, the resistances were recorded at the elevated temperature from 0 °C to 300 °C. Riekkinen and Lee reported that the variation of the resistance of TaN decreased linearly as temperature increased, indicating semiconductor-like behavior [8], [10]. The TCR values were calculated by fitting a linear curve through the resistances that were measured at the elevated temperatures from 0 °C to 300 °C. The resistance as a function of temperature is therefore,

$$R = R_0[1 + \alpha(T - T_0)] \tag{1}$$

R_0 is defined as the resistance that is measured at ambient temperature T_0 and R denotes the resistance at a heating temperature of T. Then, the temperature coefficient α can be defined as follows.

$$\alpha = [(R - R_0)/R_0]/(T - T_0) \tag{2}$$

where α is the TCR at a particular temperature. The TCR value of the TaN films is −135 ppm/°C, as shown in Fig. 5, indicating that the TCR value is relatively constant and has negative TCR with a smaller magnitude than those of conventional conducting materials (such as Pt, Cu and poly-silicon) that are utilized in ICs. Therefore, the TaN film as a micro-heater is very suitable for applications in MEMS-based metal oxide semiconductor gas sensors owing to the slight variation in its resistivity with varying temperature.

B. Measurement of Heating Properties for TaN Heater on Micro-hotplate

The maximum temperature of TaN micro-heaters with a size of 300 μm × 300 μm can exceed 500 °C. The thermal

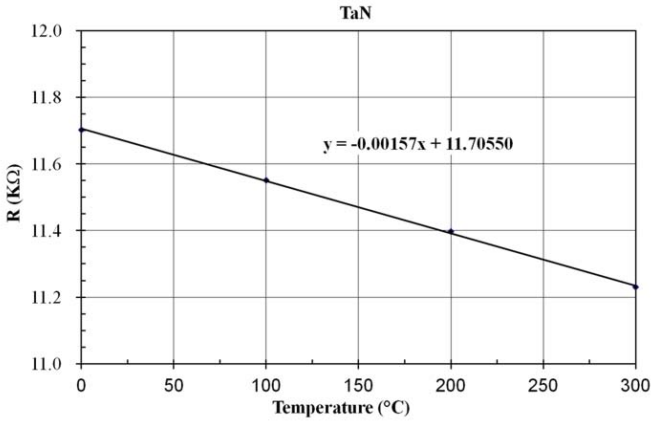

Fig. 5. Resistance versus temperature and liner regression of the TaN with a Ta/N ratio of one.

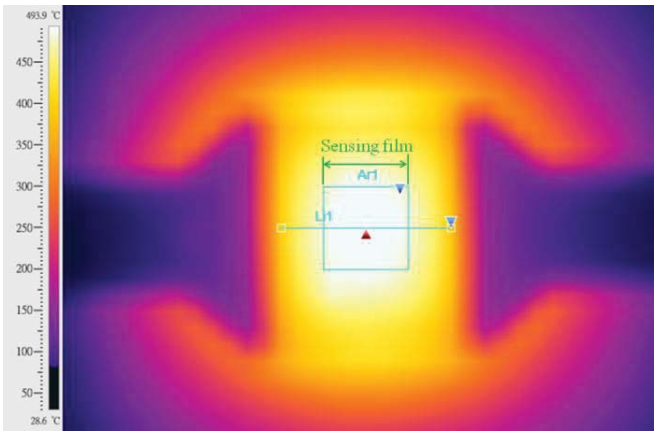

(a)

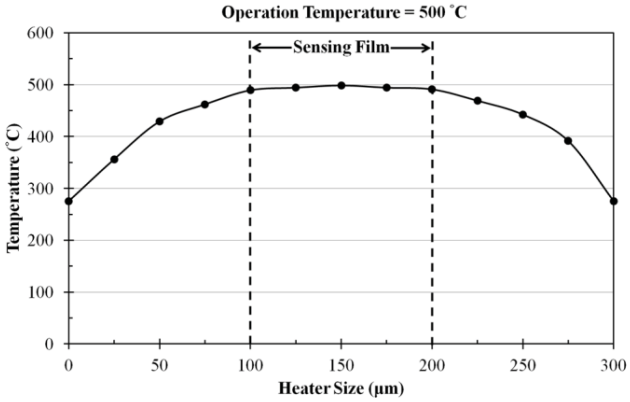

(b)

Fig. 6. Thermal distribution of the TaN micro-heater with size of 300 μm × 300 μm at 500 °C: (a) IR thermal image and (b) 1D temperature profile extracted from the IR thermal image.

distribution of the micro-heater can be determined using an IR thermometer. The IR thermometer photographs in Fig. 6(a) reveals that the heated TaN micro-heater exhibits a favorable thermal distribution on its micro-hotplate at 500 °C. In this figure, the quadrate region represents the sensing area with size of 100 μm × 100 μm and the IR imaging indicates that average temperature is around 500 °C. Fig. 6(b) plots the thermal distribution along the micro-heater which is extracted

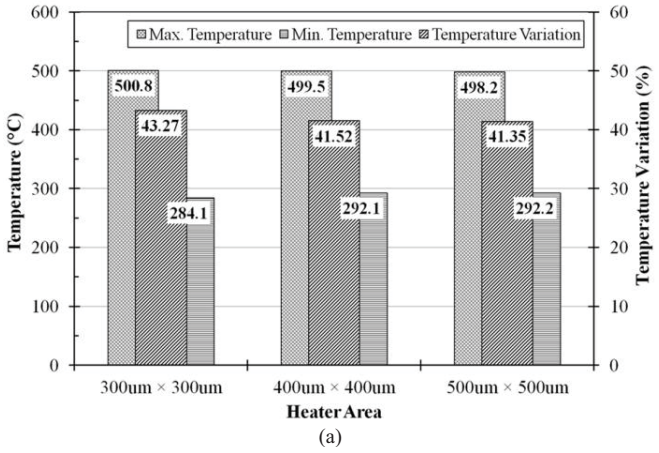

(a)

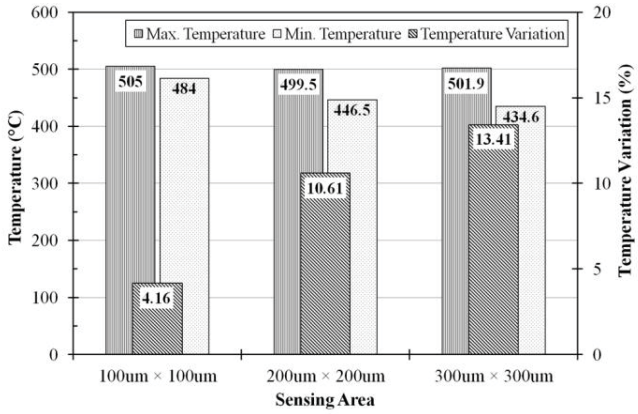

(b)

Fig. 7. Temperature response of the TaN micro-heater with different sizes operated at 500 °C: (a) heater area and (b) sensing area.

from Fig. 6(a). It shows that the maximum temperature and the minimum temperature in the sensing area are 500.7 °C and 470.1 °C, respectively. This result shows that thermal distribution in the sensing area is good homogeneous and desirable in metal oxide gas sensors since they are based in the sensitive material response at given temperature.

In this work, micro-heaters were designed with three sizes of 300 μm × 300 μm, 400 μm × 400 μm and 500 μm × 500 μm. Their thermal performance was measured using an IR thermometer at 500 °C. These measurements were used to determine the change in thermal distribution within sensing area and to find the least temperature variation for different sensing areas. Fig. 7 plots that the temperature response of the TaN micro-heater with various size operated at 500 °C. The results show that the change in temperature variation is rather significant when the micro-heater with various sizes were operated at 500 °C as shown in Fig. 7(a). However, the temperature variation over sensing area for the all designed heater is smaller as shown in Fig. 7(b). The temperature variation over the 100 μm × 100 μm sensing area is approximately 4 % at 500 °C. This result indicates that a sensing area with a size equal or less than 100 μm × 100 μm is preferred and provides a good thermal distribution.

Fig. 8 plots the power consumption of the TaN micro-heaters with various ratios of the edge length of the membrane

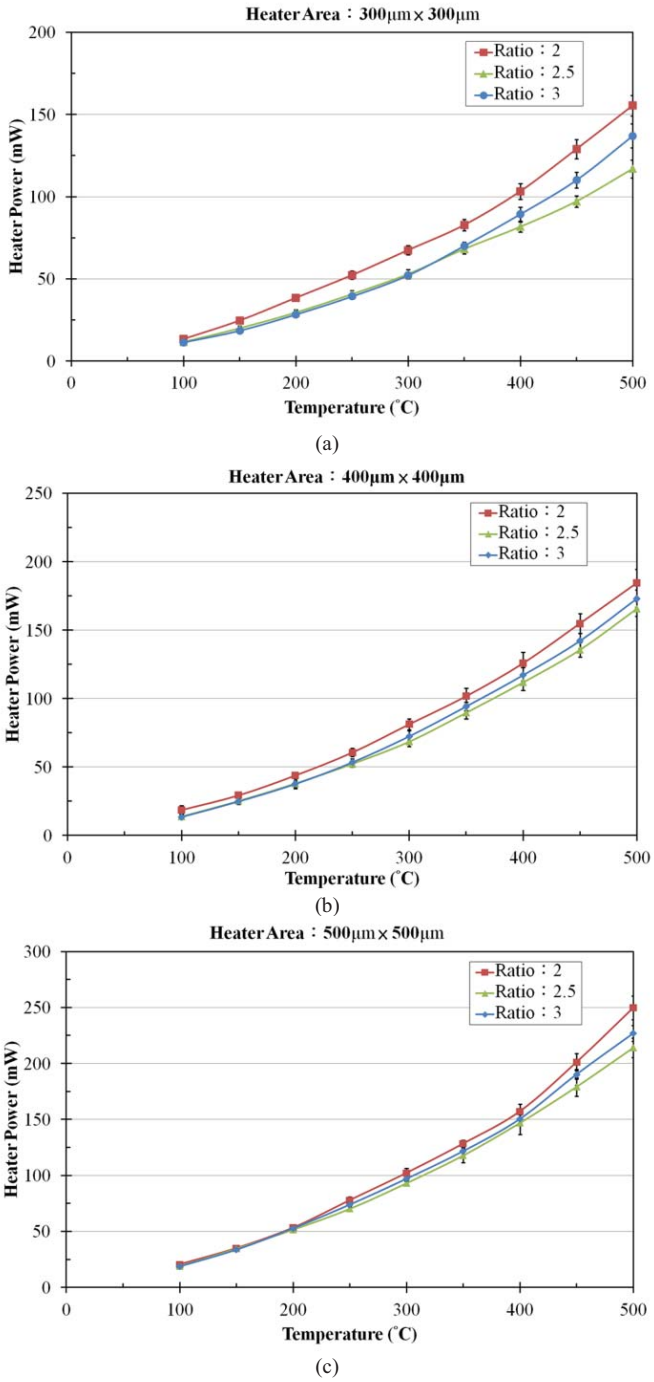

Fig. 8. Power consumption of the TaN micro-heater with various ratios of the membrane to micro-heater as a function of the operating temperature: (a) 300 μm $\times$ 300 μm heater, (b) 400 μm $\times$ 400 μm heater, and (c) 500 μm $\times$ 500 μm heater.

to that of the micro-heater against the operating temperature. The measurements show that when the ratio of the edge length of the membrane to that of the micro-heater is increased from 2 to 2.5 for the entire designed TaN heater, the power consumption of the TaN micro-heater is clearly reduced. Basically, heat is transferred by conduction, convection and radiation. According to the different pathways of heat transfer, the dissipated heat along the membrane to the silicon substrate one has to deal with heat conduction. In this study, the micro-hotplate is of the closed-membrane type, as shown in Fig. 2, whose geometry greatly affects for the heat conduction through the membrane [1]. The results in Fig. 8 demonstrate that increasing the ratio of the edge length of the membrane to that of the micro-heater effectively reduces the heat lost by heat conduction. Namely, the loss of heat by convection or radiation is rather small when the ratio of edge length was below 2.5.

As the ratio of edge lengths increases from 2.5 to 3, the power consumption of the micro-heater with size of 300 μm $\times$ 300 μm when operated in the temperature range from 100 °C to 350 °C varies little, as shown in Fig. 8(a). At 400 °C, the power consumption of the device with an edge length ratio of 3 exceeds that of the device with a ratio of 2.5 because, as the ratio increases over 2.5, the heat loss by conduction declines, and the heat loss by convection becomes dominant owing to the increase in the membrane area. That is, the heat produced from the TaN resistor on the O/N/O membrane with its low thermal conductivity flow out greatly to the surrounding air through convention mechanism. This heat transfer behavior is also evident in the micro-heaters with sizes of 400 μm $\times$ 400 μm and 500 μm $\times$ 500 μm as shown in Fig. 8(b)–(c), for which separation points in the power consumption versus operating temperature at an edge length ratio of three are reached above 250 °C and 200 °C, respectively. Table I shows that the power consumption of the TaN heater with the ratio of edge length of 2.5 and 3 at operating temperature in the separation point. In comparison to these results, shown in the Table I, the variation of power consumption for the 300 μm $\times$ 300 μm micro-heaters with 2.5 and 3 ratios is from 81.65 mW to 89.41 mW, which change more obvious than the other two. Therefore, the optimal ratio of the edge length of the membrane to that of the micro-heater is 2.5.

According to the results as mentioned above, it could be concluded that, at low temperatures, the heat losses can be completely attributed to heat conduction through the membrane, the heater material and the air, and the heater resistance versus power relationship is fairly linear. At higher temperatures the convection heat losses through the air are the most important contribution. In addition, the influence of the radiation heat losses increases with the temperature of the membrane.

Consequently, the ratio 2.5 is applied in the design of the micro-hotplate herein. The above measurements are utilized to compare the power consumed by the TaN micro-heaters of various sizes with a constant edge-length ratio of 2.5. Fig. 9 shows that the power consumption increased drastically with the increase in the size of micro-hotplate at different operating temperature, and that the change in power consumption with the temperature of the micro-heater of size 300 μm $\times$ 300 μm is smaller than those of the other two heaters. Generally, a metal oxide semiconductor gas sensor must be operated at a suitable working temperature to sense optimally, and a commonly used temperature is about 300 °C. At this operating temperature, the power consumption of a 300 μm $\times$ 300 μm micro-heater with an edge-length ratio of 2.5 is approximately 50mW.

TABLE I
THE COMPARISON OF POWER CONSUMPTION TO TaN HEATER WITH DIFFERENT RATIO OF MEMBRANE TO HEATER

Heater Size	**300 μm × 300 μm**				**400 μm × 400 μm**				**500 μm × 500 μm**			
Membrane/Heater ratio	2.5		3		2.5		3		2.5		3	
Number of Device	5		5		5		5		5		5	
Working Temperature (°C)	350	400	350	400	250	300	250	300	200	250	200	250
Average of Power Consumption (mW)	68.12	81.65	70.09	89.41	52.27	68.50	53.48	72.47	51.66	70.19	52.84	74.04
Standard Deviation (mW)	2.89	3.10	2.22	4.32	2.42	3.58	2.56	4.00	1.96	1.90	0.60	1.64

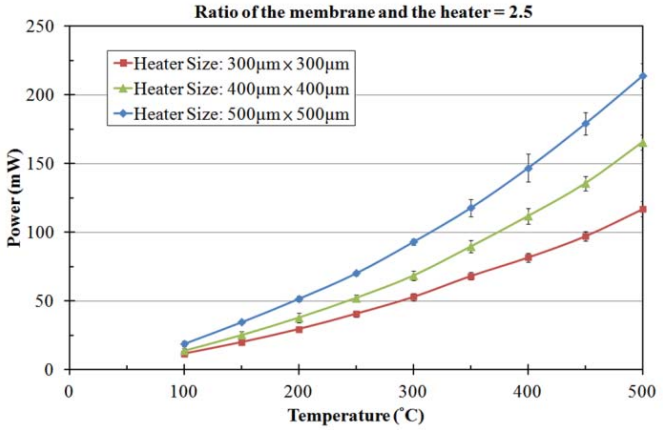

Fig. 9. The power consumption of the TaN micro-heater with various areas in a constant ratio of 2.5 as a function of different operating temperature.

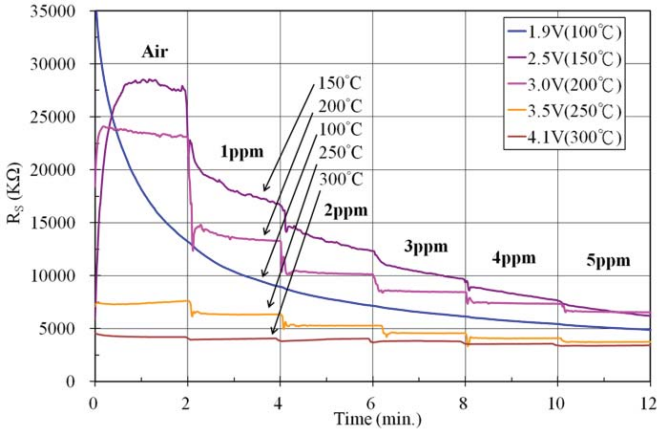

Fig. 10. The change in the R_S value of micromachined SnO_2 gas sensor with sensing area of 300 μm × 300 μm and ratio of a/b = 2.5 at various concentrations of H_2S in different operating temperature.

C. Characteristics of Response of Gas Sensors to H_2S

The gas-sensing properties of the micromachined LPD-based SnO_2 gas sensor were determined by placing the sensors in a test chamber at room temperature. Their resistance (R_a) in air was measured using a conventional circuit, in which the sensor was connected in series to an external resistor, with a circuit voltage of 1.5 V. Fig. 10 plots the responses of the micromachined SnO_2 gas sensor with a sensing area of 300 μm × 300 μm, integrated with a TaN micro-heater at different operating temperatures, to various concentrations of H_2S were obtained. Gaseous H_2S was injected into the chamber and the resistance (R_s) of the sensor was then measured. The results thus obtained show that the resistance of the gas sensor varied significantly with the concentration of H_2S gas, which was varied stepwise. The optimal working temperature of the gas sensor was obtained by using it at different operating temperatures. The results indicate that at 100 °C and 150 °C, the sensor hardly reaches equilibrium in 1 ppm of H_2S even after the elapse of 2 minutes, whereas at 250 °C it requires only some 30 seconds. On the other hand, the change in the resistance of the sensor will be reduced when the working temperature was operated at 300 °C. This difference is associated with the processes of adsorption and redox reaction on surface of sensing film and makes clear the significant dependency of sensitivity on temperature. Thus, The results in Fig. 10 show that the optimal working temperature of the gas sensor is 250 °C. Besides, The optimal working temperatures of the sensing films with sizes of 100 μm × 100 μm and 200 μm × 200 μm were similarly measured to be 300 °C and 290 °C, respectively.

Tin oxide-based gas sensors are used to detect gases at very low concentrations in the atmosphere. Their functionality depends mainly on the difference between their resistance in the presence of gaseous impurities and that in their absence. The change in sensor conductivity in the presence of reducing gases is known to be associated with the adsorption and desorption of gases, and with the redox reactions that occur on the surface of the sensing film. Hence, a relationship exists between the conductance and the concentration of the reducing gas. In this work, the sensitivity of a sensor to a gas is defined in terms of the resistance ratio:

$$S = [(R_a - R_g)/R_a] \times 100\% \tag{3}$$

where R_a and R_g are the electric resistance of the sensor electrodes before and after the introduction of a reducing gas, respectively. Since the gas sensing property of SnO_2-based sensors results from the chemisorption and/or redox reactions at the surface, and since the rates of the reactions are functions of temperature, the operating temperature of the sensor is expected to affect sensing performance. The sensitivity of each sensor to H_2S gas at staircase concentrations was measured by recording the resistance of the sensor. Fig. 11 shows that the micromachined SnO_2 gas sensor with a sensing film of size 100 μm × 100 μm is more sensitive than the other two gas sensors to H_2S gas in staircase concentrations,

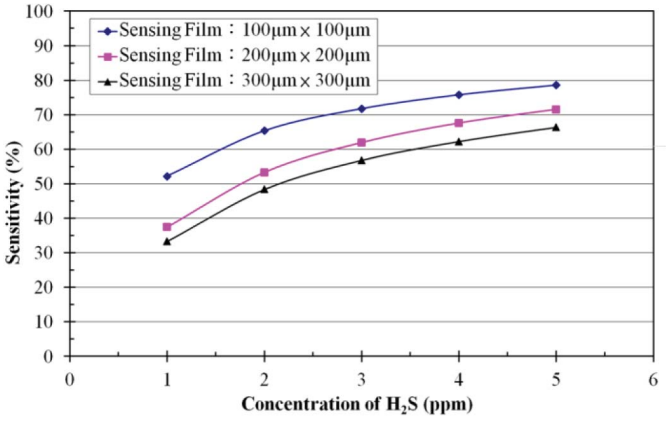

Fig. 11. The sensitivity of the micromachined SnO_2 gas sensor with various areas of sensing film in the ratio of a/b = 2.5 as a function of staircase concentration of H_2S gas.

because increasing the size of the sensing film increases the variation in temperature across the sensing area, affecting the response properties of the SnO_2 sensing film to H_2S gas. Fig. 7 shows the thermal performance is. These results suggest that a sensing film with an area of 100 μm × 100 μm or less can achieve excellent thermal distribution and good sensitivity to H_2S gas.

IV. Conclusion

A micromachined LPD-based SnO_2 gas sensor, integrated with a TaN micro-hotplate, was successfully fabricated using MEMS technology. Micro-heaters were 300 μm × 300 μm, 400 μm × 400 μm and 500 μm × 500 μm were utilized. Micro-hotplates of TaN material were heated above 500 °C and they exhibited favorable thermal distribution within the sensing area. The temperature variation over the sensing area for the TaN micro-heater of size 300 μm × 300 μm was about 4 % at 500 °C, indicating that the temperature distribution was rather uniform. The optimal ratio of the edge length of the membrane to that of the micro-heater was 2.5 since this value minimized power consumption at all operating temperatures. With respect to the gas-sensing properties of the micromachined LPD-based SnO_2 gas sensor, the optimal operating temperatures of the designed gas sensors were in the range 250 °C to 300 °C. The sensing film that was designed with a size of 100 μm × 100 μm was more sensitive to a staircase concentration of H_2S gas compared than the other two designs (200 μm × 200 μm and 300 μm × 300 μm) because the temperature variation over the sensing area is increased with the size of the sensing film. Finally, a micromachined SnO_2 gas sensor, integrated with porous sensing film that is prepared by the LPD method with a TaN micro-heater to provide heating uniformity, stable resistivity with temperature and high sensitivity to gas, was fabricated using MEMS technology.

Acknowledgment

The authors would like to thank the National Chip Implementation Center (CIC) for chip fabrication.

References

[1] I. Simon, N. Barsan, M. Bauer, and U. Weimar, "Micromachined metal oxide gas sensors: Opportunities to improve sensor performance," *Sens. Actuators, B, Chem.*, vol. 73, no. 1, pp. 1–26, Feb. 2001.

[2] S. Semancik, R. E. Cavicchi, M. C. Wheeler, J. E. Tiffany, G. E. Poirier, R. M. Walton, J. S. Suehle, B. Panchapakesan, and D. L. DeVoe, "Microhotplate platforms for chemical sensor research," *Sens. Actuators, B, Chem.*, vol. 77, nos. 1–2, pp. 579–591, 2001.

[3] M. R. T. Siregar and M. Muljono, "Design and fabrication of micro-machined gas sensors," in *Proc. IEEE Int. Conf. Semicond.*, Oct. 2006, pp. 98–101.

[4] J. Suehle, R. E. Cavicchi, M. Gaitan, and S. Semancik, "Tin oxide gas sensor using micro-hotplate by CMOS technology and in-situ processing," *IEEE Electron Device Lett.*, vol. 14, no. 3, pp. 118–120, Mar. 1993.

[5] M. Ehmann, P. Ruther, M. V. Arx, and O. Paul, "Operation and short-term drift of polysilicon-heated CMOS microstructures at temperature up to 1200 K," *J. Micromech. Microeng.*, vol. 11, no. 4, pp. 397–401, Jul. 2001.

[6] G. S. Chung and J. M. Jeong, "Fabrication of micro heaters on polycrystalline 3C-SiC suspended membranes for gas sensors and their characteristics," *Microelectron. Eng.*, vol. 87, no. 11, pp. 2348–2352, Nov. 2010.

[7] S. M. Kang, S. G. Yoon, S. J. Suh, and D. H. Yoon, "Control of electrical resistivity of TaN thin films by reactive sputtering for embedded passive resistors," *Thin Solid Films*, vol. 516, no. 11, pp. 3568–3571, 2008.

[8] T. Lee, K. Watson, F. Chen, J. Gill, D. Harmon, T. Sullivan, and B. Li, "Characterization and reliability of TaN thin film resistors," in *Proc. IEEE Int. 42nd Annu. Int. Rel.*, Apr. 2004, pp. 502–508.

[9] K. Baba and R. Hatada, "Synthesis and properties of tantalum nitride films formed by ion beam assisted deposition," *Surface Coatings Technol.*, vol. 84, no. 1, pp. 429–433, Oct. 1996.

[10] T. Riekkinen, J. Molarius, T. Laurila, A. Nurmela, I. Suni, and J. K. Kivilahti, "Reactive sputter deposition and properties of TaxN thin films," *Microelectron. Eng.*, vol. 64, no. 1, pp. 289–297, Oct. 2002.

[11] J. C. Chiou, C. Y. Lin, S. W. Tsai, and W. C. Hong, "Design and fabrication of micromachined LPD-based SnO2 gas sensor intergrated TaN with micro-hotplate," in *Proc. IEEE Sensors*, Oct. 2012, pp. 1144–1147.

[12] K. Tsukuma, T. Akiyama, and H. Imai, "Liquid phase deposition film of tin oxide," *J. Non-Cryst. Solids*, vol. 210, no. 1, pp. 48–54, Feb. 1997.

[13] A. Pike and J. W. Gardner, "Thermal modelling and characterisation of micropower chemoresistive silicon sensors," *Sens. Actuators, B, Chem.*, vol. 45, no. 1, pp. 19–26, Nov. 1997.

[14] S. W. Tsai and J. C. Chiou, "Improved crystalline structure and H2S sensing performance of CuO-Au-SnO2 thin film using SiO2 additive concentration," *Sens. Actuators, B, Chem.*, vol. 152, no. 2, pp. 176–182, 2011.

Jin-Chern Chiou received the M.S. and Ph.D. degrees in aerospace engineering science from the University of Colorado at Boulder, Boulder, CO, USA, in 1986 and 1990, respectively. Before joining the Department of Electrical and Control Engineering, National Chiao Tung University, Taiwan, in 1992, he worked at the Center for Space Structure and Control, University of Colorado, as a Research Associate. His research interests include microelectromechanical systems (MEMS), biosensors, servo control, and modeling and control of multibody dynamic systems (MBDs). Currently, he is a Professor in the Department of Electrical Engineering, National Chiao Tung University, director of the Biomedical Engineering Research and Development Center of China Medical University, and Task Force Leader of the National Science and Technology Program for SOC. He is the coauthor of Advanced Reference Books on CD-ROM System Technology and the Mechanics and Control of Large Flexible Structures. He also holds ten U.S. patents (seven pending), and eight Taiwan patents (four pending). He has received awards from the Acer Foundation, Y. Z. Hsu Foundation, Taiwan Information Storage Association (TISA), NCTU, National Science Council, Taiwan, and Chinese Institute of Engineers (Distinguished Engineering Professor Award) for his outstanding MEMS and biotechnology research.

Shang-Wei Tsai received the M.S. degree in mechanical and computer-aided engineering from Feng Chia University, Taichung, Taiwan, in 2004, and the Ph.D. degree from the Institute of Electrical and Control Engineering, National Chiao Tung University, Taiwan, in 2011. His is now a Postdoctoral Researcher in Department of Electrical Engineering, National Chiao Tung University, under supervisor Prof. J. C. Chiou. His current research interests include gas sensing performance of metal oxide semiconductor thin films, microsystem design and fabrication.

Chia-Yang Lin received the M.S. degree in electrical and control engineering from National Chiao Tung University at Hsinchu, Hsinchu, Taiwan, in 2012. He is now a Senior Engineer with United Microelectronics Corporation (UMC). His current research interests include the design and fabrication of micromachined gas sensor.